Contribution of Extreme Convective Storms to Rainfall in South America

K. L. RASMUSSEN,* M. M. CHAPLIN, M. D. ZULUAGA,+ AND R. A. HOUZE JR.

Department of Atmospheric Sciences, University of Washington, Seattle, Washington

(Manuscript received 24 April 2015, in final form 14 August 2015)

ABSTRACT

The contribution of extreme convective storms to rainfall in South America is investigated using 15 years of high-resolution data from the Tropical Rainfall Measuring Mission (TRMM) Precipitation Radar (PR). Precipitation from three specific types of storms with extreme horizontal and vertical dimensions have been calculated and compared to the climatological rain. The tropical and subtropical regions of South America differ markedly in the influence of storms with extreme dimensions. The tropical regions, especially the Amazon basin, have aspects similar to oceanic convection. Convection in the subtropical regions, centered on La Plata basin, exhibits patterns consistent with storm life cycles initiating in the foothills of the Andes and growing into larger mesoscale convective systems that propagate to the east. In La Plata basin, convective storms with a large horizontal dimension contribute ~44% of the rain and the accumulated influence of all three types of storms with extreme characteristics produce ~95% of the total precipitation in the austral summer.

1. Introduction

Precipitation from thunderstorms and mesoscale convective systems (MCSs) greatly influences agricultural and socioeconomic conditions in South America. Yet, these storms often occur in regions without routine ground-based meteorological observations. The launch of satellites with spaceborne radars has made it possible to study the physical characteristics of storms in such regions, and the Tropical Rainfall Measuring Mission (TRMM) satellite with its Precipitation Radar (PR) was in orbit long enough to evaluate these characteristics climatologically. The satellite radar's ability to discern storm structures in three dimensions makes it possible to determine the nature of the precipitating systems producing the rainfall. Using these radar data to study the frequency, intensity, and structure of extreme precipitation events in the current climate will lay groundwork for anticipating changes in these patterns of precipitating convection as climate changes occur.

It is important to examine the climatology of storm type as well as rainfall. In general, regions experiencing the most precipitation typically do not coincide with regions known to support storms with the most extreme vertical structure (Zipser et al. 2006). Hence, flash flooding and severe local weather may be favored despite low overall rainfall. On the other hand, MCSs (Houze 2004), characterized as storms with large horizontal dimensions, can contribute large fractions of warm season rainfall because of their breadth, long-lived nature, and repeated occurrence in certain regions (Fritsch et al. 1986; Durkee et al. 2009). It therefore seems important to determine the climatology of convective storms with differing horizontal and vertical scales.

The goal of this study is to assess the relative contribution of precipitation from storms with the most extreme horizontal and vertical dimensions to the climatological precipitation in South America. Some past studies have focused on the contributions to rainfall by systems of different horizontal dimension (e.g., Liu 2011; Romatschke and Houze 2013). Other studies have examined the statistics of vertical echo structure (e.g., Boccippio et al. 2005). In the present study, we use a technique that uses metrics of both vertical and horizontal dimensions to identify deep convective systems of different types, corresponding to different stages of

* Current affiliation: National Center for Atmospheric Research, Boulder, Colorado.

+ Current affiliation: Universidad Nacional de Colombia, Medellín, Colombia.

Corresponding author address: Kristen Lani Rasmussen, National Center for Atmospheric Research, 3450 Mitchell Lane, Boulder, CO 80301.
E-mail: kristenr@ucar.edu

DOI: 10.1175/JHM-D-15-0067.1

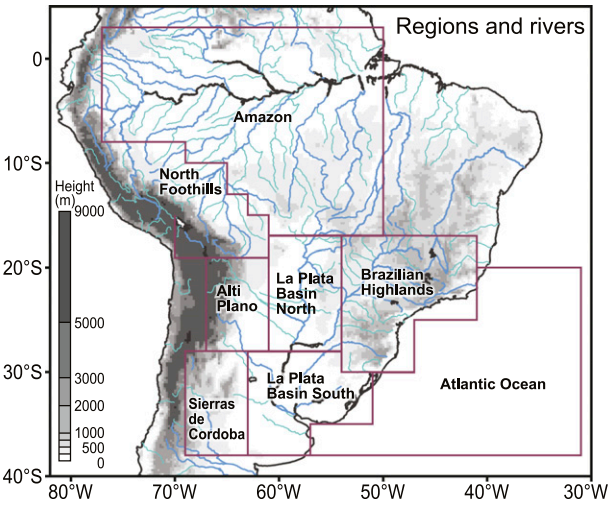

FIG. 1. Topographical map of South America showing the Andes mountain range, associated terrain features, and major rivers. Selected regions for this study are outlined in maroon and labeled.

convective system development. Romatschke and Houze (2010), Rasmussen and Houze (2011), and Rasmussen et al. (2014) have used this methodology to examine climatological patterns of convection across South America. These studies showed how the storms vary regionally in character. However, these studies did not determine the contribution from storms of different types and in different stages of development to the rainfall climatology of the continent. That is the purpose of this paper.

2. Data and methodology

a. *Regions of study*

For reference, Fig. 1 shows the regions examined in this study as well as the major rivers in South America. Our methodology identifies the contributions by different storm types in the indicated regions.

b. *Identification of extreme echo features and storm types*

The TRMM PR has fine three-dimensional spatial resolution (4–5 km horizontal, 250 m vertical) with a near-uniform quasi-global coverage that permits comprehensive analysis between 36°N and 36°S (Kummerow et al. 1998, 2000). This study uses 15 years of TRMM PR, version 7 (V7), data from January 1998 to December 2012 for the austral spring through fall seasons. We focus on the austral spring [September–November (SON)] and summer [December–February (DJF)] to specifically address the impact of storms with extreme characteristics on warm season convective precipitation. Additionally, Houze et al. (2015) demonstrate that in regions experiencing frequent midlatitude frontal systems during the winter, stratiform echoes are more likely to be produced by frontogenetical processes rather than having their origin in convective processes. Thus, we limit the focus of this study to the seasons most likely to experience convective storms and MCSs in South America. The following TRMM data products are used:

- 2A23 (rain characteristics; Awaka et al. 1997), where rain is separated into three categories: convective, stratiform, and other, and all references to convective and stratiform precipitation are based on these classifications; and
- 2A25 (rainfall rate and profile; Iguchi et al. 2000), which provides the attenuation-corrected three-dimensional reflectivity data.

These data were processed following the methodology of Houze et al. (2007) and Romatschke et al. (2010). All of the fields were mapped onto a 0.05° × 0.05° latitude–longitude Cartesian grid. We first identify all three-dimensional echo objects that have detectable radar reflectivity consisting of two or more contiguous horizontal pixels. Each such object is defined as a distinguishable rain area (DRA; Houze et al. 2015).

All pixels located in DRAs are identified, and the precipitation rates in those pixels are calculated. We search each DRA to determine if it contains embedded within it certain extreme characteristics. The embedded features that we identify here have been defined and used in previous studies of continental convection by Houze et al. (2007), Romatschke and Houze (2010), Romatschke et al. (2010), Houze et al. (2011), Rasmussen and Houze (2011), Rasmussen et al. (2013, 2014, 2015), Zuluaga and Houze (2015), Rasmussen and Houze (2015, manuscript submitted to *Mon. Wea. Rev.*), and Houze et al. (2015). These embedded features are defined as 1) deep convective core (DCC), which is a three-dimensional contiguous 40-dBZ echo ≥10 km in maximum height; 2) wide convective core (WCC), which is a three-dimensional contiguous 40-dBZ echo with a maximum horizontal dimension ≥1000 km^2; and 3) broad stratiform region (BSR), which is a region of contiguous stratiform echo ≥50 000 km^2 in horizontal dimension. These embedded echo features have a relationship to the stage of development of the storm producing the echoes. DCCs represent especially intense convection and tend to be found in earlier stages of development. WCCs represent very intense convection that has grown upscale to form a mesoscale unit of intense convection. BSRs occur in the mature and later stages of development of MCSs (Houze 2004). Using ground-based radar, Zuluaga and Houze (2013) demonstrated that these types of echo features indeed

represent early, middle, and later stages of convective system development in a statistical sense.

We define ''storm type'' according to whether a DRA contains one of the categories of embedded extreme echo features (DCC, WCC, or BSR). If so, then the DRA is referred to as a storm containing a DCC, WCC, or BSR. Then, we determine whether or not the rain observed by the TRMM PR at a given location and time was falling from a DRA containing one of the above echo types. The main objective of the paper is to compile rainfall statistics on storms containing DCCs, WCCs, and BSRs. We have also defined a separate category of storms containing both DCCs and WCCs. However, for conciseness we have not included this combined category in some of the maps presented below. Suffice it to say that those mapped patterns lie between those of storms containing DCCs and WCCs, and we will present summary statistics that include this combined category.

c. Precipitation estimation

Iguchi et al. (2009) suggested that the TRMM PR V7 2A25 rainfall algorithm tends to underestimate the precipitation from deep convection over land. Rasmussen et al. (2013) investigated the scope of this bias in extreme storms in South America and confirmed that the TRMM PR V7 2A25 algorithm tends to underestimate rain in all three extreme echo types used in the current study because of insufficiencies in the rain algorithm in capturing the full characteristics of deep convective storms over land regions. Rasmussen et al. (2013) showed that lower estimates by the algorithm are most biased for extreme precipitating systems that contain significant mixed phase and/or frozen hydrometeors. Regions of South America that experience the most frequent storms containing deep convective cores are in the subtropics that do not regularly receive large amounts of climatological rainfall. Thus, an underestimation of the climatological precipitation can influence the perception of the climatology and hydrologic cycle in South America.

To mitigate the TRMM PR algorithm bias for the types of overland storms studied here, we adopted the methodology of Rasmussen et al. (2013), who proposed using the Z–R relationship

$$Z = aR^b, \tag{1}$$

where Z is the equivalent radar reflectivity factor ($\mathrm{mm^6\,m^{-3}}$) and R is the rain rate ($\mathrm{mm\,h^{-1}}$). This relationship is used to estimate surface precipitation from the TRMM PR attenuation-corrected reflectivity data. The lowest nonzero value of Z is used at each data pixel between the surface and 2.5 km above ground level for each precipitation echo, which is similar to the procedure used for the TRMM PR algorithm 2A25 (Rasmussen et al. 2013). The parameters a and b are constants depending on rain type (convective, stratiform, or other). Rasmussen et al. (2013) examined multiple values for these parameters. Here we use values used previously by Romatschke and Houze (2011), which give a reasonable estimate of precipitation in the tropics and subtropics (convective: $a = 100$, $b = 1.7$; stratiform: $a = 200$, $b = 1.49$; and other: $a = 140$, $b = 1.6$).

d. Calculation of storm type rain contribution

One complication in using the TRMM PR data to develop statistics of rainfall by certain storm types is that the sampling by satellite overpasses is intermittent in time and space (Negri et al. 2002). For statistics to be comparable between locations, we must make an accommodation for the irregular sampling. To make the data comparable, we define a parameter F to be applied to every horizontal grid element (pixel):

$$F = \left(\frac{N_S}{N_T}\right), \tag{2}$$

where N_T is the total number of times a given pixel is sampled by a TRMM overpass and N_S is the number of times that pixel is occupied by a certain storm type (defined in section 2b) at the time of an overpass. The contribution C of a given storm type to the rainfall at that pixel is then calculated according to

$$C = F\left(\frac{\overline{R}_S}{\overline{R}_T}\right), \tag{3}$$

where $\overline{R}_T$ is the average rain rate ($\mathrm{mm\,h^{-1}}$) seen in a given pixel over the 15 years of TRMM measurements and $\overline{R}_S$ is the average rain rate within the subset of those grid elements that are occupied by a given storm type. The resulting values represent a satellite overpass-corrected field of the rain contribution from each storm type to the total precipitation in the study region. By using this technique, this study will assess how much of the climatological rain is contributed by each extreme storm type and provide insights into the influence of extreme-storm-related precipitation on the hydrologic cycle in various regions of South America.

3. Background climatology of precipitation and radar echo characteristics

a. South American hydroclimate

The hydroclimate of South America varies strongly from the tropical to subtropical regions. Tropical South

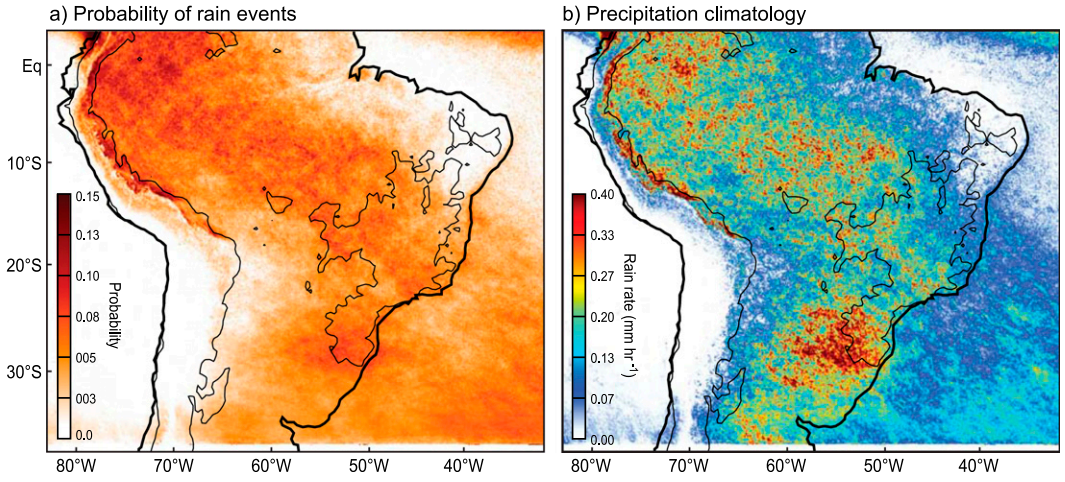

FIG. 2. (a) Geographical distribution of the probability of finding a DRA (≥2 pixels) during the austral spring (SON) from 1998 to 2012. (b) Precipitation climatology for all DRAs identified in (a). The contour inside the continent represents the 500-m terrain elevation.

America, largely characterized by the Amazon River basin, has a pronounced annual cycle of precipitation that supports the largest rain forest in the world and contributes 20% of the global river freshwater discharge to oceans (Richey et al. 1989). Seasonal variations of the intertropical convergence zone (ITCZ) and South Atlantic convergence zone (SACZ) result in wet and dry seasons in tropical South America in the summer and winter, respectively (Kodama 1992; Nogués-Paegle and Mo 1997; Carvalho et al. 2004). In contrast, subtropical South America, largely characterized by La Plata River basin, receives much less precipitation than the tropical regions in general, but the precipitation variability in the spring and summer is related to the occurrence of both deep convection and MCSs in this region (Velasco and Fritsch 1987; Zipser et al. 2006; Salio et al. 2007; Romatschke and Houze 2011; Rasmussen and Houze 2011; Houze et al. 2015).

The Andes mountain range affects the hydroclimate of both tropical and subtropical South America. As one of the largest and longest mountain ranges on Earth, the Andes influence the exchange of moisture and heat from the tropical to subtropical regions primarily through the South American low-level jet (SALLJ; Vera et al. 2006) along the eastern foothills of the Andes. Deep convection in subtropical South America is related to the presence of the SALLJ (Salio et al. 2007; Rasmussen and Houze 2011; Rasmussen and Houze 2015, manuscript submitted to *Mon. Wea. Rev.*). In addition, the relationship between steep-sloping terrain and heavy rainfall is particularly important for the susceptibility to both flash and slow-rise river flooding and agricultural sustainability in subtropical South America (Latrubesse and Brea 2009). This investigation of the hydroclimate characteristics in tropical and subtropical South America, specifically focused on the most extreme precipitation elements seen by the TRMM satellite, is important for understanding the hydrometeorology in South America with implications for forecasting, agriculture, human consumption, hydropower, streamflow characteristics in tropical versus subtropical river basins, and future climate projections.

b. *TRMM radar echo characteristics*

Figure 2 shows the probability of finding a DRA during the austral spring (i.e., SON; Fig. 2a) and the climatology of precipitation generated by these events (Fig. 2b). Although the precipitation maps shown in Fig. 2b and throughout this study are created with TRMM PR orbital data (i.e., instantaneous measurements with TRMM PR over an orbital swath), the spatial patterns of rainfall in these 15-yr-long samples are in agreement with climatologies of precipitation relying on continuous and merged multisensor measurements (e.g., Huffman et al. 2001; Rozante et al. 2010; Liu 2015). In the austral spring, more DRAs tend to occur in the tropical Amazon basin than the subtropics, particularly near the Andes foothills (Fig. 2a). The precipitation climatology for the spring shows an especially robust rain maximum in southern Brazil and northeastern Argentina, likely related to frequent MCSs in this region. Rasmussen et al. (2014) examined the lightning and severe storm characteristics of storms in the austral spring and showed that maxima in lightning flash rates and flood storm reports are collocated with the rain maximum seen in Fig. 2b, likely related to storms with both deep and wide intense convective characteristics.

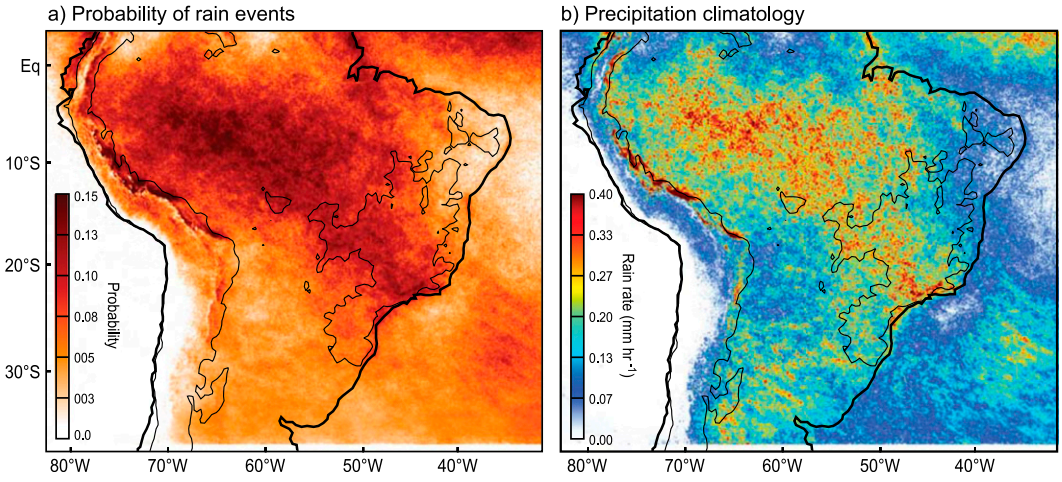

FIG. 3. As in Fig. 2, but for the austral summer (DJF).

Figure 3 shows similar maps for the austral summer (i.e., DJF). The contrast between the tropics and subtropics regarding the number of DRAs is much greater than for the austral spring (Fig. 3a). The Amazon basin has a large amount of climatological rain contributed by many raining events in the region. However, the subtropics receive a substantial amount of rainfall despite the low number of events there compared to the tropics. Similar to the austral spring (Fig. 2), the subtropical rainfall is produced by fewer events than tropical rainfall. Additionally, the subtropical region exhibits a distinct longitudinal shift in the probability of DRAs and the climatological precipitation to the west toward the Andean foothills. A similar shift in extreme storm occurrence and lightning production is shown in Rasmussen et al. (2014), consistent with convective initiation and upscale growth into MCSs in subtropical South America (Romatschke and Houze 2010; Rasmussen and Houze 2011; Rasmussen and Houze 2015, manuscript submitted to *Mon. Wea. Rev.*).

Figure 4 presents an overview of the probability of finding the three categories of extreme radar echo structures with the TRMM satellite (defined in section 2b) for both the spring and summer. DCCs are notably absent in the tropical Amazon (Figs. 4a,d). WCCs and BSRs do occur in the Amazon region, though not as frequently as in the subtropics. Comparing to Figs. 2 and 3 and a recent study examining the variable nature of convection globally from TRMM PR data (Houze et al. 2015), we conclude that the convective elements in this region have a less deep maritime-like character, consistent with Mohr et al. (1999), but nevertheless can aggregate into mesoscale units and overall contribute a large amount of precipitation in the Amazon basin. This characteristic of convection being weaker but nevertheless productive of rainfall verifies the frequently made claim that the Amazon region is climatologically similar to a tropical ocean; sometimes this characterization is referred to as the Amazon region being a "green ocean." The Amazon region has large expanses of open water, a moist and shallow boundary layer, and limited surface temperature variability. Recent studies have demonstrated that mesoscale variations in surface heating are an important factor for convective intensity variability over oceans and continents (Robinson et al. 2011). Additionally, Wall et al. (2014) show that the absence of strong low-level wind shear and convergence in tropical South America contributes to the maritime character of the Amazon. Figure 4 is an objective verification of this oceanic characteristic of Amazon convective precipitation. Houze et al. (2015) show that the lack of DCC echoes, especially in summer (Fig. 4d), and the frequent occurrence of BSR echoes (Fig. 4f) are characteristics similar to those seen over the tropical oceans.

The regions with the highest probability of extreme echo occurrence in the subtropics are collocated with the maximum in precipitation in the spring and summer. Previous studies of subtropical South American convective systems in the austral summer have hypothesized a storm life cycle where convection initiates along the Andean foothills and sometimes grows upscale into MCSs while propagating east or northeast and then decays into broad stratiform regions farther east (Romatschke and Houze 2010; Matsudo and Salio 2011; Rasmussen and Houze 2011). The storm type distributions of DCCs, WCCs, and BSRs in spring are heavily concentrated in southern Brazil and northeastern Argentina, unlike the summer patterns. This difference suggests that a somewhat different canonical storm life cycle occurs during the austral spring and should be investigated in a future

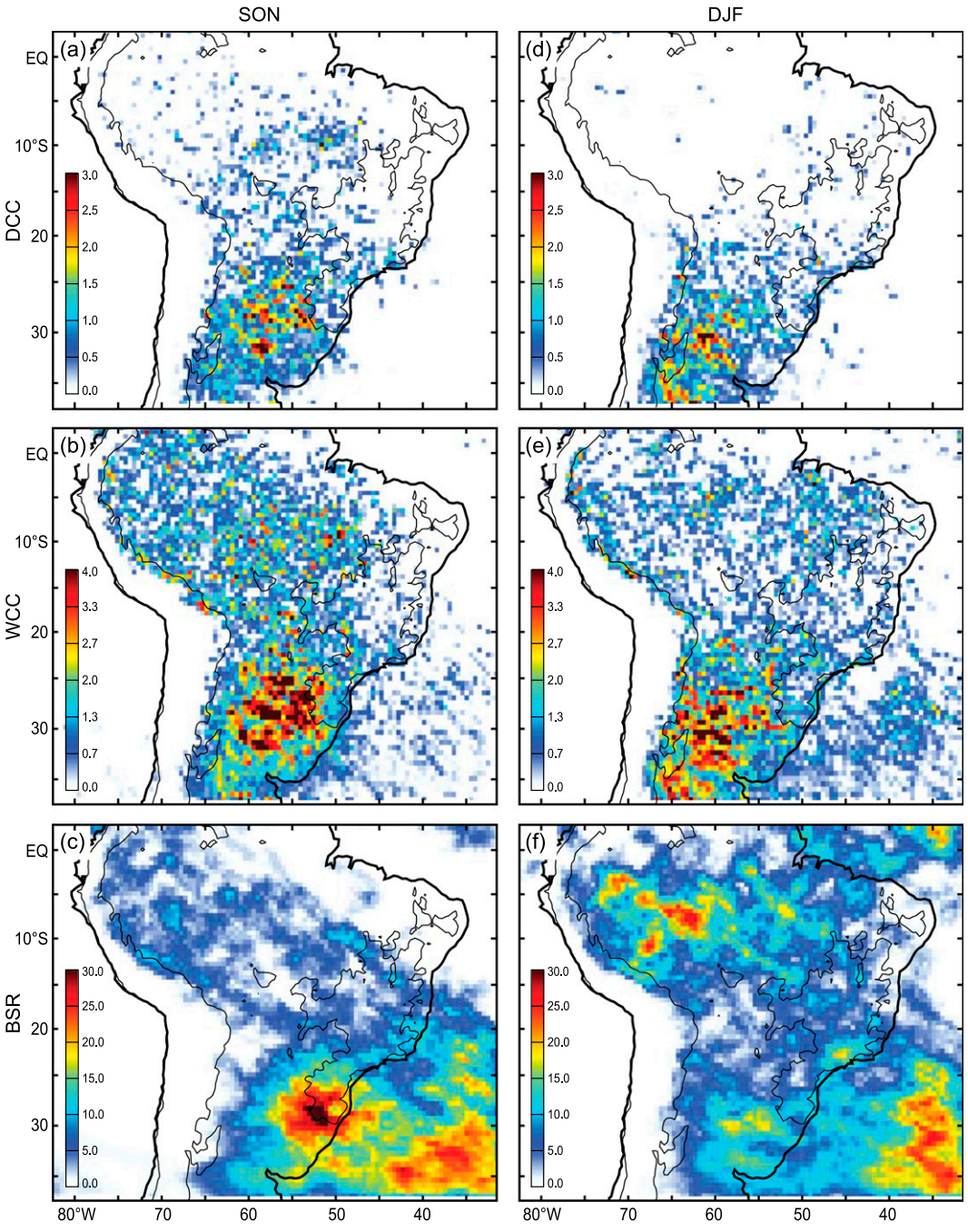

FIG. 4. Geographical distribution of the probability of finding an event by each extreme type during the austral (left) spring (SON) and (right) summer (DJF) from 1998 to 2012. The contour inside the continent represents the 500-m terrain elevation.

study. However, as will be discussed below in section 5, an analysis of the diurnal cycle of extreme-storm-contributed rainfall in both the spring and summer show similar eastward propagation and upscale growth from the late afternoon through early morning, but with decreased magnitudes in the spring.

Table 1 shows the overall statistics of the total number of DRAs and TRMM-identified extreme echo cores (defined in section 2b) for the austral spring through fall seasons, identified in each region defined by the boxes in Fig. 1. In general, more storms containing WCCs were identified in most of the regions. However, the ratio of

TABLE 1. Number of extreme echo cores and DRAs identified in each of the study regions.

	Altiplano	Amazon	Atlantic	Brazilian Highlands	Northern La Plata	Southern La Plata	Northern foothills	Sierras de Córdoba
DCCs	346	427	76	535	403	638	97	1019
WCCs	341	2389	1585	1182	898	2315	620	1049
BSRs	22	572	1466	327	103	514	112	44
DRAs	57 150	715 435	610 958	191 789	50 045	123 712	183 614	64 714

the number of extreme cores to the total DRAs is very low (Table 2). The highest percentages of extreme storms to total events are WCCs in the northern and southern La Plata regions (1.8% and 1.9%, respectively) that experience frequent MCSs in the spring and summer. As seen in Table 3 showing the average size of the embedded extreme echoes in various regions in South America, WCCs cover a much larger area than DCCs and thus likely contribute more precipitation. Thus, ~2% of the storms in La Plata basin likely make up a large fraction of the climatological rain, echoing the discussion of Figs. 2 and 3 above. This type of assessment of how much rain each storm type contributes provides crucial information for water management and extreme-storm-related flood risks in subtropical South America.

4. Rainfall contributions by storms containing extreme radar echo structures

We now examine the contributions of the precipitation produced by various types of storms on South American hydroclimate. A "storm type" is assigned to a DRA (as defined in section 2b) if it contains an embedded extreme echo of one or more of the types defined in section 2b as DCC, WCC, and BSR. For the precipitation at a pixel to be attributed to one of these storm types, the rain falling must be from a DRA that contains one of these three extreme elements. Figures 5 and 6 represent the spatial distribution of the rainfall contribution C, defined in (3), to the total rain by storm types containing DCCs, WCCs, and BSRs during the austral spring and summer, respectively.

Overall, storms containing WCCs are the strongest contributors to the climatological rainfall in South America in both spring and summer (Figs. 5b, 6b). Storms containing DCCs have a moderately strong impact in southwestern Argentina (Fig. 6a), but otherwise contribute relatively little to total rainfall. The storms with DCCs are smaller in horizontal scale and shorter lived than storms that contain WCCs or BSRs. In the subtropical zone, the precipitation contribution from storms containing BSRs tends to maximize just east of the region where storms containing WCCs are most frequent, consistent with the hypothesis that storms grow and decay as they propagate eastward (Romatschke and Houze 2010; Matsudo and Salio 2011; Rasmussen and Houze 2011). The rain contributions by storms with wide cores are of extreme importance in the subtropical spring, most notably over La Plata basin, where the maximum of WCC occurrence and precipitation are collocated (cf. Figs. 4b, 5b). Storms containing WCCs have both very intense rainfall and have organized up to a larger horizontal scale. Thus, they have the double advantage of heavy rain elements and large area.

Consistent with the southwestward shift from the spring to summer of extreme echo type probability (Fig. 4), the rain contributions for each storm type also shift southwestward toward the Andean foothills during summer (Fig. 6). Storms with DCCs contribute slightly more rain to the total compared to spring, and the pattern is focused around the Sierras de Córdoba (small north–south secondary mountain feature east of the main Andes barrier between ~30° and 35°S) in Fig. 6a, suggesting stronger orographic forcing in the summer. Similar to Fig. 5, storms containing WCCs contribute the most climatological rain in the subtropics near central Argentina and Uruguay. This region is important to the hydroclimate of South America because frequent extreme MCSs occur here (Romatschke and Houze 2010; Rasmussen and Houze 2011; Rasmussen et al. 2014; Rasmussen and Houze 2015, manuscript submitted to *Mon. Wea. Rev.*). Rasmussen et al. (2014) showed a

TABLE 2. Ratio of the number of extreme echo cores to the total number of DRAs in each of the study regions, expressed as a percentage (%).

	Altiplano	Amazon	Atlantic	Brazilian Highlands	Northern La Plata	Southern La Plata	Northern foothills	Sierras de Córdoba
DCCs	0.60	0.06	0.01	0.28	0.80	0.51	0.05	1.56
WCCs	0.59	0.33	0.26	0.62	1.79	1.86	0.34	1.61
BSRs	0.04	0.08	0.24	0.17	0.21	0.42	0.06	0.07

TABLE 3. Averaged areas (km^2) of DRAs containing extreme echo cores in each of the study regions.

	Altiplano	Amazon	Atlantic	Brazilian Highlands	Northern La Plata	Southern La Plata	Northern foothills	Sierras de Córdoba
DCCs	26 766	15 259	54 724	30 117	46 201	48 207	19 865	25 049
WCCs	53 491	42 399	68 497	60 502	70 807	70 411	46 668	40 367
BSRs	96 932	96 914	105 116	108 182	114 625	112 548	98 774	101 126

similar southwestward shift in the occurrence of flooding events in the spring-to-summer transition associated with the same storm types examined in this study. Both flash and slow-rise floods have been associated with extreme events producing large amounts of rainfall; thus, this study is consistent with the findings of Rasmussen et al. (2014). In both the spring and summer, Figs. 5 and 6 clearly show that the dominant contribution to the total rain is by storms containing WCCs in subtropical South America.

Some studies have focused on a narrow maximum of climatological rain along the Andes foothills in the northern foothills region (labeled in Fig. 1; Garreaud 1999; Mohr et al. 2014). This feature is evident in Figs. 2 and 3. However, Figs. 5 and 6 show no significant precipitation along the northern foothills by storms containing extreme radar echoes. This result implies that the narrow maximum of precipitation along the northern foothills must be due to smaller or weaker nonextreme echoes that likely form repeatedly in frequent uplift of warm tropical air by low-level easterly winds consistently impinging on the tropical Andes foothills. A full characterization of the storms in the tropical Andes foothills is beyond the scope of this study but will be explored in future work.

a. Regional rainfall contributions

Figure 7 shows the accumulated precipitation contributions for each storm type and region in the spring and summer, expressed as percentages. The designation DWCC indicates contributions by storms containing both DCCs and WCCs (section 2b). Consistent with Figs. 5 and 6, the contribution from storms with extreme characteristics to the climatological precipitation is very small in tropical compared to subtropical South America (Fig. 7). As previously shown in Figs. 4b, 4c, 5b, and 5c, the austral spring shows patterns of robust WCCs in east-central Argentina and BSRs located farther east along the southwestern edge of the Brazilian Highlands. The rain contributions in Fig. 7 echo these results and show the importance of storms containing BSRs in the austral spring. However, along the subtropical Andes foothills, the spring and summer rain contributions are very similar (Fig. 7), indicating the strong orographic control on storms with extreme characteristics in the immediate lee of the Andes during both seasons.

Storms with wide convective cores contribute more rain than other extreme storm categories in all of the continental precipitation regions in the austral summer, consistent with higher ratios of WCC events to DRAs in Table 2. The variations in contribution by storms with DCCs, WCCs, and BSRs to the total rain in the subtropics during the austral summer are consistent with the storm life cycle hypothesis from Romatschke and Houze (2010), Matsudo and Salio (2011), and Rasmussen and Houze (2011) discussed in section 3. Higher percentages from storms with DCCs in the Altiplano and Sierras de Córdoba regions along the Andes foothills highlight the role of terrain features in focusing convective initiation, as has been recently demonstrated via mesoscale modeling in Rasmussen and Houze (2015, manuscript submitted to *Mon. Wea. Rev.*). Farther east over La Plata basin, storms with DCCs contribute less rain, while the contributions from storms with WCCs to the total rain are ~10%–15% higher than in the Sierras de Córdoba region because of upscale growth and intensification of convective systems during the austral summer. Moving farther east where MCSs tend to decay and become more stratiform in nature, contributions by storms with DCCs and WCCs decrease over the Atlantic Ocean. BSR contributions increase from low values near the foothills out to the Atlantic Ocean.

The southern La Plata basin region shows the highest contribution from storms with extreme characteristics. A total of ~43% of the summer rain falls from storms with WCCs. Given that La Plata basin is the fifth-largest river basin in the world, having ~43% of its warm season rainfall come from an extreme storm type typically associated with MCSs demonstrates the considerable role of storms with WCCs on the hydrologic cycle in subtropical South America. Approximately 95% of the total summer rain in the southern La Plata basin region is accounted for by contributions of storms with extreme convective and stratiform elements (i.e., storms containing DCCs, WCCs, DWCCs, or BSRs). Table 2 shows that storms with extreme characteristics in the southern La Plata basin region make up only ~3% of all raining events in this region. Thus, ~3% of all events are responsible for producing ~70% of the spring precipitation

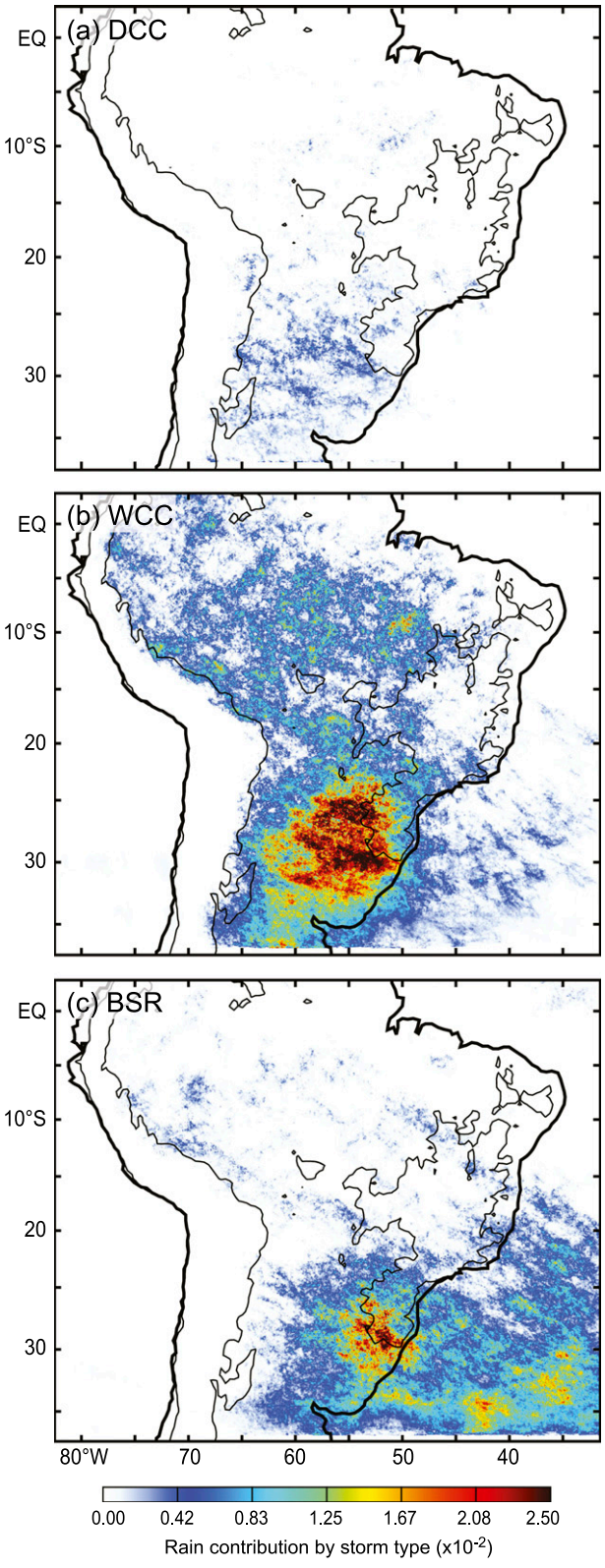

FIG. 5. Geographical distribution of the rainfall contribution to the total rain by each storm type during the austral spring (SON) from 1998 to 2012. The contour inside the continent represents the 500-m terrain elevation.

and ~95% of the summer precipitation in the southern La Plata basin region. The importance of understanding the character of storms contributing these very large fractions of precipitation is an important area for future study.

In contrast to subtropical South America, the more maritime nature of the precipitation in tropical South America (Houze et al. 2015) does not promote the generation of deep or intense convective systems on a regular basis (Figs. 5, 6). The contribution from storms with extreme embedded features to the total rainfall in the tropics is therefore relatively low compared to the subtropics (Fig. 7). Rain contributions in the northern foothills and Amazon regions are surprisingly similar given their differential proximity to the Andes. One exception is storms containing WCCs in the austral spring, whose proximity to the Andes affects the magnitude of their rain contribution. However, the influence of the Andes is much stronger in the subtropics because of the relationship to convective storm initiation and development (Romatschke and Houze 2010; Rasmussen and Houze 2011; Rasmussen et al. 2014; Rasmussen and Houze 2015, manuscript submitted to *Mon. Wea. Rev.*).

b. Seasonal variability

Figure 8 shows a monthly time series of the accumulated rain contribution from the three storm types (i.e., storms containing DCCs, WCCs, and BSRs) in the northern foothills and Amazon (Fig. 8a) and the southern La Plata basin and Sierras de Córdoba regions (Fig. 8b), expressed as percentages. Overall, the rain contributions from extreme storms in the tropics are lower, consistent with a maritime-like regime with typically smaller and less intense convection (Houze et al. 2015). Over the progress of the seasons, the relative rain contributions from each storm type are comparable, suggesting that the more maritime nature of convection continues throughout the spring and summer (Fig. 8a). The two subtropical regions (Fig. 8b) also exhibit similarities in the storm type rain contribution percentages, with a notable maximum in contributions by storms containing DCCs and WCCs in the summer months (i.e., DJF). In contrast, storms containing BSRs are minimum in summer, likely indicating the presence of fewer frontal systems to enhance the stratiform echoes in subtropical South America during that season.

5. Diurnal cycle

To assess the impact of the diurnal cycle on the rain contributions from storms with extreme characteristics, time–longitude diagrams representing the diurnal progression of rain contribution are presented in Fig. 9 during the austral summer. The data are averaged over a

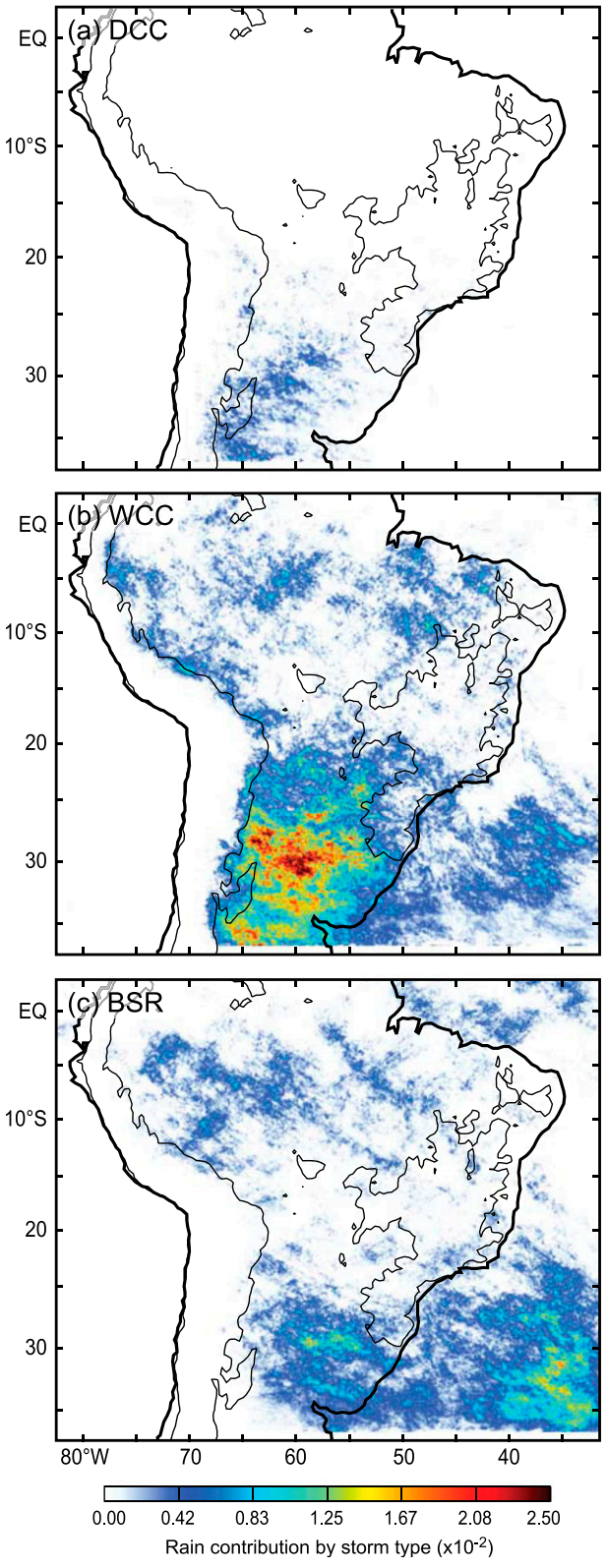

FIG. 6. As in Fig. 5, but for the austral summer (DJF).

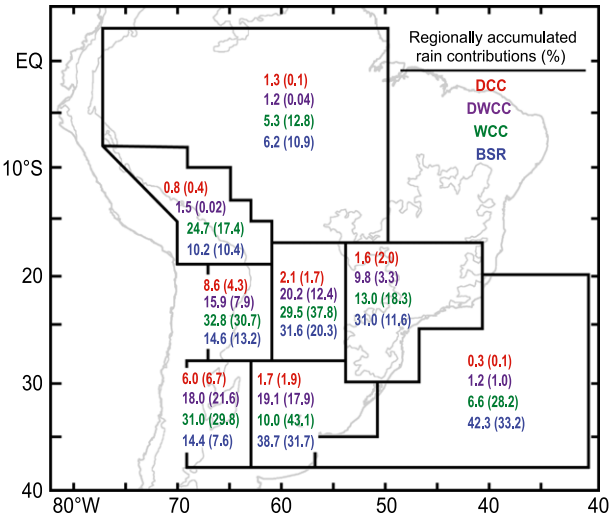

FIG. 7. Percentage of the accumulated rainfall contribution from each storm type (indicated by the colors in the legend) to the total accumulated precipitation in each region. Values on the left represent the contribution from the austral spring (SON), while the ones in parentheses are from the austral summer (DJF).

meridional band bounded by 36°–28°S, which was chosen because it includes La Plata basin and Sierras de Córdoba. Storms containing DCCs initiate around 1400 local time near the Andean foothills, which is consistent with solar heating of the Andes combined with the SALLJ bringing moisture south from the Amazon to provide a favorable environment for deep convection (Velasco and Fritsch 1987; Zipser et al. 2006; Romatschke and Houze 2010; Rasmussen and Houze 2011; Matsudo and Salio 2011; Rasmussen et al. 2014; Rasmussen and Houze 2015, manuscript submitted to *Mon. Wea. Rev.*). In Fig. 9a, the black contours represent the rain contribution from storms containing DCCs only, indicating the strong tendency for such systems to appear at the time of initiation of convection in the immediate foothills of the Andes. The eastward-propagating pattern in Fig. 9a thus indicates how the DCC and WCC echo characterizations relate to each other in a diurnal time-sequential sense. The observed behavior is that storms containing DCCs form at initiation but then grow upscale after initiation to form storms of mesoscale dimension that contain WCCs as they propagate eastward. This behavior is consistent with that hypothesized by Romatschke and Houze (2010), Matsudo and Salio (2011), and Rasmussen and Houze (2011).

As storms containing DCCs move eastward, growing upscale into intense WCCs, they contribute more climatological precipitation over the plains beyond the foothills (Figs. 9a,b). By late evening to early morning, the MCSs are more developed and contain WCCs that

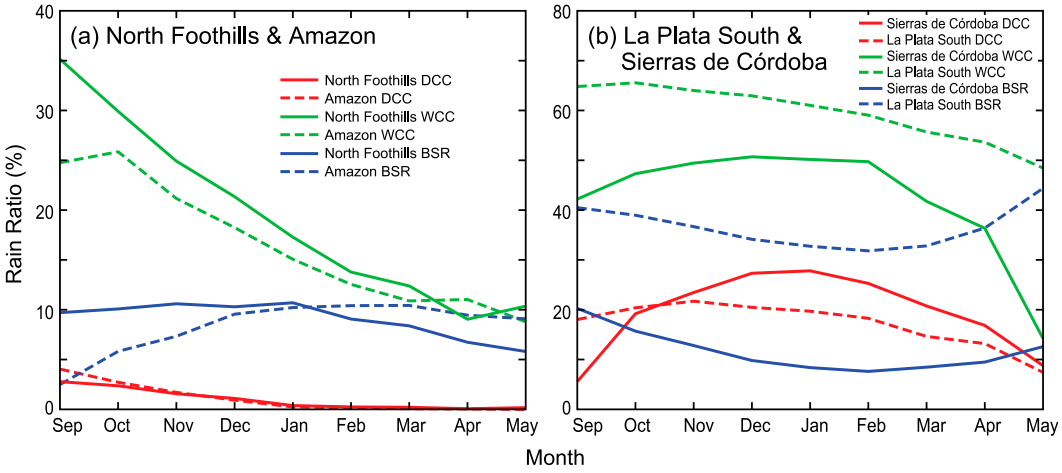

FIG. 8. Monthly time series of the accumulated rain contribution, expressed as percentages, from the three storm types (DCC, WCC, and BSR) in the regions of the (a) northern foothills and Amazon and (b) southern La Plata and Sierras de Córdoba regions.

are nocturnal, cover large areas on average, and tend to last ~18 h, as suggested by the TRMM observations (Figs. 9a,b). As the convective elements within the storms containing WCCs begin to lose their buoyancy in their mature phase, they transition into stratiform precipitation. Figure 9c shows that this transition occurs in the early morning and persists through midday. However, a sharp cutoff in the precipitation at the edge of the continent (i.e., ~50°W) indicates that the storms significantly weaken as they move off the coast and over the Atlantic Ocean. Figure 9 echoes the results of studies investigating the diurnal characteristics and longitudinal propagation of MCS-related precipitation over the United States forming near another major mountain range (i.e., the Rockies) and moving eastward (Trier et al. 2010).

Rasmussen et al. (2014) recently found that the diurnal patterns of extreme-storm-related lightning exhibit a convective back-building tendency toward the Andes. Storms containing DCCs only (black contours in Fig. 9a) show a tendency for the most intense convective elements to remain linked with the Andes foothills from the initiation stage through the early morning hours, in agreement with the back-building hypothesis of Rasmussen et al. (2014). However, the categories associated with larger and more organized convection (color shading in Figs. 9a–c) show a clear eastward propagation as MCSs grow, expand, and move eastward during their diurnal life cycle. Thus, while the convective intensity along the Andes foothills remains strong from the early afternoon through the early morning [Fig. 3 in Rasmussen et al. (2014); Fig. 9a], the precipitation associated with the eastward-expanding MCSs moves eastward. A time–longitude diagram representing the diurnal cycle of precipitation from all summertime DRA events seen by the TRMM satellite is presented in Fig. 10. A strikingly similar diurnal cycle of precipitation is revealed when comparing Figs. 9 and 10, further supporting the dominant nature of extreme storms and mesoscale convective systems in the hydroclimate of subtropical South America.

6. Conclusions

This investigation using 15 years of TRMM PR data provides insights into the influence of convective systems with extreme characteristics on the hydrologic cycle in South America. TRMM satellite observations have enabled an unprecedented characterization of South American precipitation because most of the continent is sampled frequently with the same instrumentation and because the TRMM PR measures the vertical as well as horizontal structure of the radar echoes of precipitating convection. To assess the relative contribution to climatological rainfall by the most extreme configurations over the continent, precipitation was accumulated from all raining pixels seen by the TRMM satellite. By identifying those particular types of extreme radar echo structures that are considered to approximate the life cycle stages of extreme convective systems, from newly developed to mature to decaying, we have been able to map the ratio of extreme-storm-contributed rain in each of its stages to the continent's climatological rain. From a hydrologic and climatological viewpoint, this empirical knowledge is useful because the type of runoff and flooding that may occur depends on the specific character and life stage of the convection and precipitation reaching the surface and

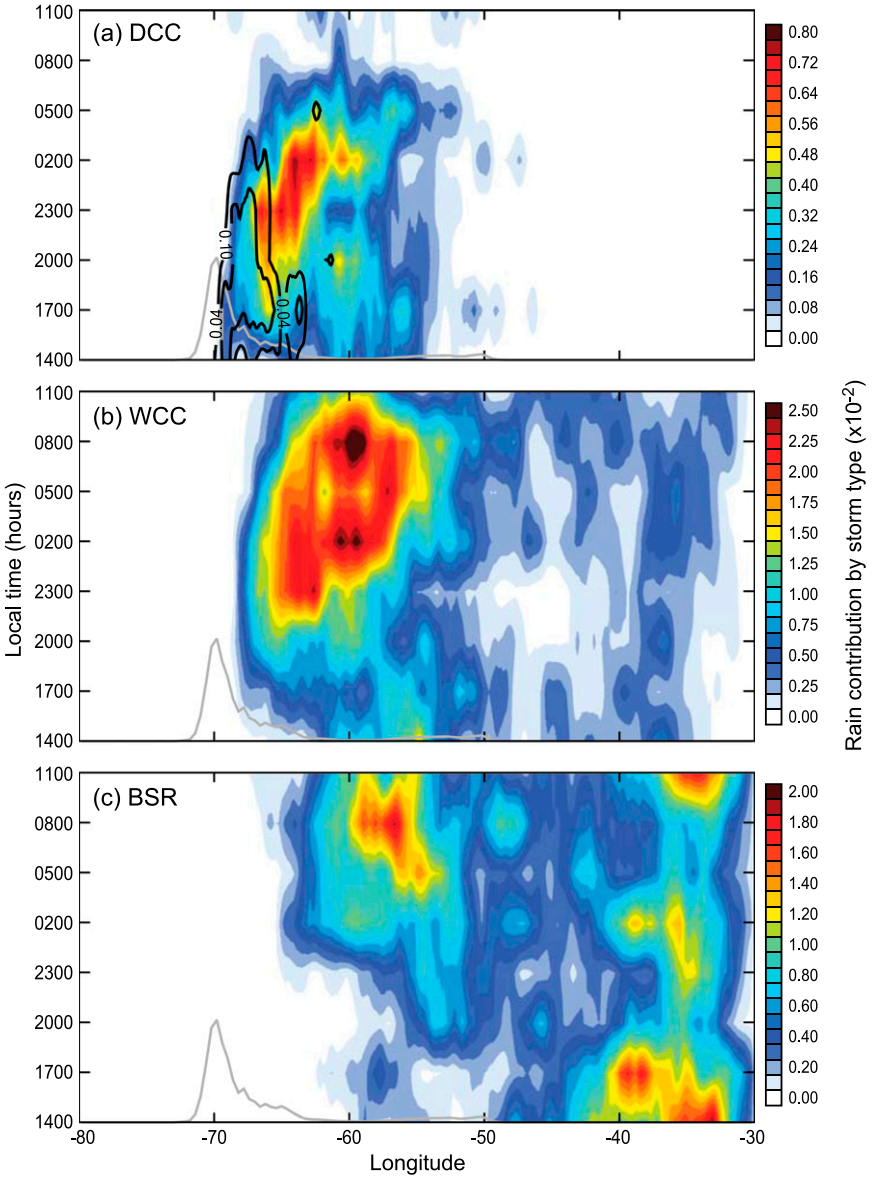

FIG. 9. Time–longitude diagrams representing the diurnal progression of the contribution to the total rain climatology from (a) DCCs, (b) WCCs, and (c) BSRs for the austral summer (DJF). The black contour in (a) is the contribution from those events that were classified as DCC only (see text). The diagrams are averaged over a meridional band bounded by 36°–28°S. The gray line in (a)–(c) represents the average topographic relief between 36° and 28°S with a max height of 3500 m.

has broad implications for the hydrological cycle in this region.

An algorithm applied to the TRMM PR data has identified three distinct categories of storms containing embedded echoes of extreme horizontal or vertical dimension from the TRMM PR data. A significant difference in how much rain storms containing these forms of embedded echoes contribute to the climatological rain in the tropics and subtropics of South America reveals the different characteristics of the convective populations in these two climatological regimes. Table 4 shows the relative impact of precipitation from storms with extreme characteristics in the tropics and subtropics of South America during the austral spring and summer. Although tropical South America has a higher number of events and more climatological rain, the relative impact of total extreme storm precipitation on the hydrologic cycle of the Amazon is a factor of 2–3

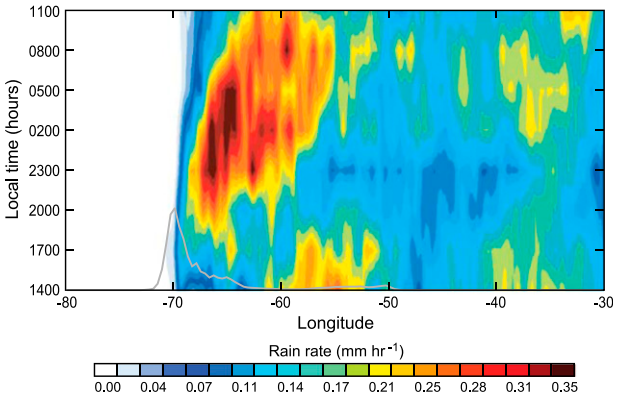

FIG. 10. As in Figs. 9a–c, but for the climatological diurnal cycle of precipitation (mm h^{-1}) from all DRAs in subtropical South America during the austral summer (DJF).

lower than the subtropics. The tropical region of South America, primarily the Amazon basin, maintains a generally maritime character with relatively few extreme events yet abundant precipitation. In contrast, the subtropics, primarily Argentina, have much less rain, but that rain is explained almost wholly by storms of the most extreme categories. The subtropical rainstorms are strongly controlled by the Andes. For these reasons, the role of extreme storms on the hydrologic cycle is markedly different between the tropics and subtropics of South America.

In the subtropical zone of South America, storms containing deep convective cores contribute only a small proportion of climatological rain near the foothills because of their smaller size and typically short-lived and relatively infrequent nature. Storms containing wide convective cores contribute a large fraction of the climatological rain in La Plata basin, as they are typically associated with growing and mature mesoscale convective systems that are large in area and tend to be long-lived systems. Storms containing broad stratiform regions contribute a significant amount of climatological rain with decaying mesoscale convective systems with widespread and long-lived stratiform precipitation. In La Plata basin, storms containing wide convective cores contribute ~44% of the total warm season rain. The accumulated contribution from storms containing deep convective cores, deep and wide convective cores, wide convective cores, and broad stratiform regions is ~95% of the total warm season precipitation in La Plata basin. In La Plata basin, storms with extreme characteristics only make up ~3% of the total events that occur, so although these storms are rare, they produce most of the rain. Since such a large fraction of the total warm season precipitation is associated with storm types related to the life cycle of strong MCSs, local populations and the regional economy critically depend on these types of storms.

TABLE 4. Climatological rain contribution from DRAs containing extreme echo cores to the climatological rain in the tropical and subtropical regions of South America during the austral spring and summer.

	Tropics (%)	Subtropics (%)
DCCs	1.4/0.5	1.6/1.9
DCCs and WCCs	2.3/0.5	11.2/9.8
WCCs	24.5/13.8	34.5/33.2
BSRs	9.5/10.4	38.4/26.9
Total rain contribution	39.1/25.2	85.7/83.5

Diurnal time–longitude analysis of the rain contribution by these three types of storms in the subtropical zone in summer is consistent with the mesoscale convective system life cycle hypothesis from Romatschke and Houze (2010), Matsudo and Salio (2011), and Rasmussen and Houze (2011). Convective initiation in the late afternoon near the foothills of the Andes sometimes leads to the upscale growth of convective echoes to form nocturnal mesoscale convective systems that begin to expand eastward and then finally decay into broad stratiform regions farther east. As mentioned in Rasmussen et al. (2014) and Rasmussen and Houze (2015, manuscript submitted to *Mon. Wea. Rev.*), the most intense convective elements have a back-building character that tend to remain tied to the terrain from the late afternoon hours during convective initiation through the mature stages of the storm in the early morning hours. This pattern contrasts with the precipitation associated with larger convection that moves diurnally in a continuous eastward shift along with the growing systems.

Convective storms with extreme characteristics have the greatest impact in La Plata basin in South America. Given that La Plata basin produces ~70% of the gross national product for countries within the basin (Mechoso et al. 2001; World Water Assessment Program 2009), major rivers in the basin supply ~80% of the electricity to the region through hydroelectric power, and it is the fifth-largest river basin in the world, an understanding of the storms that contribute 70%–95% of the rainfall associated with convective storms in the region is extremely important. Changes in the timing, frequency, location, or intensity of the mesoscale convective systems would have considerable practical implications. In the future, a greater understanding of the relationship of how much of the hydrologic cycle of South America depends on storms with the specific convective and mesoscale characteristics described in this paper will provide valuable information on the hydroclimate of the region. Modeling for forecasting of weather and floods is challenged by the variety

of storm structures and life cycles occurring over different parts of the continent. As climate changes, these convective behaviors and patterns may change, and accurate modeling will be needed to assess potential changes. In the present climate, better information is needed for local water management, high-impact weather mitigation, and the scientific understanding of the hydrometeorology of South America with implications for hydrological forecasting and public safety. This study lays groundwork for such advances.

Acknowledgments. The authors thank Edward Zipser and two anonymous reviewers for their comments and suggestions, which have greatly improved this manuscript. Beth Tully coordinated the graphics. This research was sponsored by NSF Grant AGS-1144105, NASA Grants NNX13AG71G and NNX10AH70G, and a NASA Earth and Space Science Graduate Fellowship (NNX11AL65H).

REFERENCES

Awaka, J., T. Iguchi, H. Kumagai, and K. Okamoto, 1997: Rain type classification algorithm for TRMM Precipitation Radar. *IGARSS '97: Remote Sensing—A Scientific Vision for Sustainable Development*, Vol. 4, IEEE, 1633–1635, doi:10.1109/IGARSS.1997.608993.

Boccippio, D. J., W. A. Petersen, and D. J. Cecil, 2005: The tropical convective spectrum. Part I: Archetypal vertical structures. *J. Climate*, **18**, 2744–2769, doi:10.1175/JCLI3335.1.

Carvalho, L. M. V., C. Jones, and B. Leibmann, 2004: The South Atlantic Convergence Zone: Form, persistence, and relationships with intraseasonal and interannual activity and extreme rainfall. *J. Climate*, **17**, 88–108, doi:10.1175/1520-0442(2004)017<0088:TSACZI>2.0.CO;2.

Durkee, J. D., T. L. Mote, and J. M. Shepherd, 2009: The contribution of mesoscale convective complexes to rainfall across subtropical South America. *J. Climate*, **22**, 4590–4605, doi:10.1175/2009JCLI2858.1.

Fritsch, J. M., R. J. Kane, and C. R. Chelius, 1986: The contribution of mesoscale convective weather systems to the warm-season precipitation in the United States. *J. Climate Appl. Meteor.*, **25**, 1333–1345, doi:10.1175/1520-0450(1986)025<1333:TCOMCW>2.0.CO;2.

Garreaud, R. D., 1999: Multiscale analysis of the summertime precipitation over the central Andes. *Mon. Wea. Rev.*, **127**, 901–921, doi:10.1175/1520-0493(1999)127<0901:MAOTSP>2.0.CO;2.

Houze, R. A., Jr., 2004: Mesoscale convective systems. *Rev. Geophys.*, **42**, RG4003, doi:10.1029/2004RG000150.

——, D. C. Wilton, and B. F. Smull, 2007: Monsoon convection in the Himalayan region as seen by the TRMM Precipitation Radar. *Quart. J. Roy. Meteor. Soc.*, **133**, 1389–1411, doi:10.1002/qj.106.

——, K. L. Rasmussen, S. Medina, S. R. Brodzik, and U. Romatschke, 2011: Anomalous atmospheric events leading to the summer 2010 floods in Pakistan. *Bull. Amer. Meteor. Soc.*, **92**, 291–298, doi:10.1175/2010BAMS3173.1.

——, ——, M. D. Zuluaga, and S. R. Brodzik, 2015: The variable nature of convection in the tropics and subtropics: A legacy of 16 years of the Tropical Rainfall Measuring Mission (TRMM) satellite. *Rev. Geophys.*, **53**, 994–1021, doi:10.1002/2015RG000488.

Huffman, G. J., R. F. Adler, M. M. Morrissey, D. T. Bolvin, S. Curtis, R. Joyce, B. McGavock, and J. Susskind, 2001: Global precipitation at one-degree daily resolution from multisatellite observations. *J. Hydrometeor.*, **2**, 36–50, doi:10.1175/1525-7541(2001)002<0036:GPAODD>2.0.CO;2.

Iguchi, T., R. Meneghini, J. Awaka, T. Kozu, and K. Okamoto, 2000: Rain profiling algorithm for the TRMM Precipitation Radar data. *Adv. Space Res.*, **25**, 973–976, doi:10.1016/S0273-1177(99)00933-3.

——, T. Kozu, J. Kwiatkowski, R. Meneghini, J. Awaka, and K. Okamoto, 2009: Uncertainties in the rain profiling algorithm for the TRMM Precipitation Radar. *J. Meteor. Soc. Japan*, **87A**, 1–30, doi:10.2151/jmsj.87A.1.

Kodama, Y., 1992: Large-scale common features of subtropical precipitation zones (the Baiu frontal zone, the SPCZ, and the SACZ). Part I: Characteristics of subtropical frontal zones. *J. Meteor. Soc. Japan*, **70**, 813–835.

Kummerow, C., W. Barnes, T. Kozu, J. Shiue, and J. Simpson, 1998: The Tropical Rainfall Measuring Mission (TRMM) sensor package. *J. Atmos. Oceanic Technol.*, **15**, 809–817, doi:10.1175/1520-0426(1998)015<0809:TTRMMT>2.0.CO;2.

——, and Coauthors, 2000: The status of the Tropical Rainfall Measuring Mission (TRMM) after two years in orbit. *J. Appl. Meteor.*, **39**, 1965–1982, doi:10.1175/1520-0450(2001)040<1965:TSOTTR>2.0.CO;2.

Latrubesse, E. M., and D. Brea, 2009: Floods in Argentina. *Natural Hazards and Human-Exacerbated Disasters in Latin America*, E. Latrubesse, Ed., Developments in Earth Surface Processes, Vol. 13, Elsevier, 333–349, doi:10.1016/S0928-2025(08)10016-5.

Liu, C., 2011: Rainfall contribution from precipitation systems with different sizes, intensities, and durations. *J. Hydrometeor.*, **12**, 394–412, doi:10.1175/2010JHM1320.1.

Liu, Z., 2015: Comparison of precipitation estimates between version 7 3-hourly TRMM Multi-Satellite Precipitation Analysis (TMPA) near-real-time and research products. *Atmos. Res.*, **153**, 119–133, doi:10.1016/j.atmosres.2014.07.032.

Matsudo, C. M., and P. V. Salio, 2011: Severe weather reports and proximity to deep convection over northern Argentina. *Atmos. Res.*, **100**, 523–537, doi:10.1016/j.atmosres.2010.11.004.

Mechoso, R. C., and Coauthors, 2001: Climatology and hydrology of the Plata basin. VAMOS Scientific Study Group on the Plata Basin Doc., 56 pp. [Available online at http://www.atmos.umd.edu/~berbery/lpb/science_plan.html.]

Mohr, K. I., J. S. Famiglietti, and E. J. Zipser, 1999: The contribution to tropical rainfall with respect to convective system type, size, and intensity estimated from the 85-GHz ice-scattering signature. *J. Appl. Meteor.*, **38**, 596–606, doi:10.1175/1520-0450(1999)038<0596:TCTTRW>2.0.CO;2.

——, D. Slayback, and K. Yager, 2014: Characteristics of precipitation features and annual rainfall during the TRMM era in the central Andes. *J. Climate*, **27**, 3982–4001, doi:10.1175/JCLI-D-13-00592.1.

Negri, A. J., T. L. Bell, and L. Xu, 2002: Sampling of the diurnal cycle of precipitation using TRMM. *J. Atmos. Oceanic Technol.*, **19**, 1333–1344, doi:10.1175/1520-0426(2002)019<1333:SOTDCO>2.0.CO;2.

Nogués-Paegle, J., and K. C. Mo, 1997: Alternating wet and dry conditions over South America during summer. *Mon. Wea. Rev.*, **125**, 279–291, doi:10.1175/1520-0493(1997)125<0279:AWADCO>2.0.CO;2.

Rasmussen, K. L., and R. A. Houze Jr., 2011: Orogenic convection in South America as seen by the TRMM satellite. *Mon. Wea. Rev.*, **139**, 2399–2420, doi:10.1175/MWR-D-10-05006.1.

——, S. L. Choi, M. D. Zuluaga, and R. A. Houze Jr., 2013: TRMM precipitation bias in extreme storms in South America. *Geophys. Res. Lett.*, **40**, 3457–3461, doi:10.1002/grl.50651.

——, M. D. Zuluaga, and R. A. Houze Jr., 2014: Severe convection and lightning in subtropical South America. *Geophys. Res. Lett.*, **41**, 7359–7366, doi:10.1002/2014GL061767.

——, A. J. Hill, V. E. Toma, M. D. Zuluaga, P. J. Webster, and R. A. Houze, Jr., 2015: Multiscale analysis of three consecutive years of anomalous flooding in Pakistan. *Quart. J. Roy. Meteor. Soc.*, **141**, 1259–1276, doi:10.1002/qj.2433.

Richey, J. E., L. A. K. Mertes, T. Dunne, R. L. Victoria, B. R. Forsberg, A. C. N. S. Tancredi, and E. Oliveira, 1989: Sources and routing of the Amazon River flood wave. *Global Biogeochem. Cycles*, **3**, 191–204, doi:10.1029/GB003i003p00191.

Robinson, F. J., S. C. Sherwood, D. Gerstle, C. Liu, and D. J. Kirshbaum, 2011: Exploring the land–ocean contrast in convective vigor using islands. *J. Atmos. Sci.*, **68**, 602–618, doi:10.1175/2010JAS3558.1.

Romatschke, U., and R. A. Houze Jr., 2010: Extreme summer convection in South America. *J. Climate*, **23**, 3761–3791, doi:10.1175/2010JCLI3465.1.

——, and ——, 2011: Characteristics of precipitating convective systems in the South Asian monsoon. *J. Hydrometeor.*, **12**, 3–26, doi:10.1175/2010JHM1289.1.

——, and ——, 2013: Characteristics of precipitating convective systems accounting for the summer rainfall of tropical and subtropical South America. *J. Hydrometeor.*, **14**, 25–46, doi:10.1175/JHM-D-12-060.1.

——, S. Medina, and R. A. Houze Jr., 2010: Regional, seasonal, and diurnal variations of extreme convection in the South Asian region. *J. Climate*, **23**, 419–439, doi:10.1175/2009JCLI3140.1.

Rozante, J. R., D. S. Moreira, L. G. de Goncalves, and D. A. Vila, 2010: Combining TRMM and surface observations of precipitation: Technique and validation over South America. *Wea. Forecasting*, **25**, 885–894, doi:10.1175/2010WAF2222325.1.

Salio, P., M. Nicolini, and E. J. Zipser, 2007: Mesoscale convective systems over southeastern South America and their relationship with the South American low-level jet. *Mon. Wea. Rev.*, **135**, 1290–1309, doi:10.1175/MWR3305.1.

Trier, S. B., C. A. Davis, and D. A. Ahijevych, 2010: Environmental controls on the simulated diurnal cycle of warm-season precipitation in the continental United States. *J. Atmos. Sci.*, **67**, 1066–1090, doi:10.1175/2009JAS3247.1.

Velasco, I., and J. M. Fritsch, 1987: Mesoscale convective complexes in the Americas. *J. Geophys. Res.*, **92**, 9591–9613, doi:10.1029/JD092iD08p09591.

Vera, C., and Coauthors, 2006: The South American Low-Level Jet Experiment. *Bull. Amer. Meteor. Soc.*, **87**, 63–77, doi:10.1175/BAMS-87-1-63.

Wall, C., E. J. Zipser, and C. Liu, 2014: An investigation of the aerosol indirect effect on convective intensity using satellite observations. *J. Atmos. Sci.*, **71**, 430–447, doi:10.1175/JAS-D-13-0158.1.

World Water Assessment Program, 2009: Water in a changing world. United Nations World Water Development Rep. 3, UNESCO Publishing, 318 pp.

Zipser, E. J., C. Liu, D. J. Cecil, S. W. Nesbitt, and D. P. Yorty, 2006: Where are the most intense thunderstorms on Earth? *Bull. Amer. Meteor. Soc.*, **87**, 1057–1071, doi:10.1175/BAMS-87-8-1057.

Zuluaga, M. D., and R. A. Houze Jr., 2013: Evolution of the population of precipitating convective systems over the equatorial Indian Ocean in active phases of the Madden–Julian oscillation. *J. Atmos. Sci.*, **70**, 2713–2725, doi:10.1175/JAS-D-12-0311.1.

——, and ——, 2015: Extreme convection of the near-equatorial Americas, Africa, and adjoining oceans as seen by TRMM. *Mon. Wea. Rev.*, **143**, 298–316, doi:10.1175/MWR-D-14-00109.1.